An Evaluation on Seismic Behavior of VRF Damper by Shaking Table Test

JANG Jeong-Hyun, HWANG Ji-Hoon & CHOI, Jae-Hyouk†
Chosun University, Korea

KAMIYA Takashi
Yahagi Construction CO., LTD, Japan

OH Sang-Hoon
Pusan National University, Korea

SUMMARY:
The Shear-type Variable Resistance Friction (VRF) Damper is developed to effectively respond to a variety of seismic motions to have different frictional forces within the friction damper that has remarkable energy absorption ability. In order to evaluate the seismic performance of the Shear-type VRF Damper, tests by shaking table were carried out. For these tests, two (2) Shear-type VRF Dampers were installed with low force of 30kN and higher force of 80kN to the SDOF structure and the characteristics of its dynamic behavior were investigated in order to apply following seismic wave to El-Centro and Kobe. The test result shows that the Shear-type VRF Damper with improved existing friction damper could effectively resist both small and big earthquakes. Furthermore, the test result is compared with the result of numerical analysis on the Shear-type VRF Damper.

Keywords: Variable Resistance Friction (VRF) Damper, Shaking table test, Seismic performance

1. INTRODUCTION

Dampers are used commonly as a means to mitigate structures' excessive response to earthquakes. In order to minimize damages to the structures by absorbing their vibration energy through dissipation of hysteretic behaviors, the damper is very effective in seismic design of the building structures. Among these dampers, the friction damper has a low dependent on temperature or frequency and has a stable hysteretic behavior to the repeated load. This is the reason why it is widely used. Of design variables of the friction damper, initial stiffness and slip resistance can be easily set using the friction surface and the introductory tension. In addition, the friction damper has a relatively simple energy dissipation mechanism and it is easy to manufacture and install.

Filatrault and Cherry proposed a method to design the friction damper that can minimize the displacement response and the amount of energy dissipation, taking into consideration such variables as proper cycle of the structures, frequency components of the excitation load, and slip resistance. Moreschi and Singh proposed optimal slip load and brace stiffness required for designing the friction damper, using the optimization technique. In order to apply the friction damper to the seismic design of structures, it is necessary to determine design variables like initial stiffness and slip resistance based on response behaviors of the structures. The conventional friction damper is applied to the structures, with its slip resistance set to have the greatest vibration control effect for the estimated earthquake vibration level. However, once the initial slip resistance is set to the friction damper, the friction damper does not slip when an earthquake vibration lower than the estimated earthquake vibration is received and thus does not absorb the vibration energy. On the contrary, it may slip excessively for strong earthquake vibration, making it unable to protect the structure from vibration.

In this study, therefore, the dynamic behaviors of Variable Resistance Friction (VRF) Damper developed to effectively react to various types of earthquake vibration were investigated with setting the same friction damper to have different friction resistances. For this, VRF Damper having both low-resistance part and high-resistance part was installed inside a structure of Single Degree of Freedom (SDOF), using a large vibration table on which earthquake vibrations could be simulated. Then, El-Centro and Kobe earthquake waves were excited to investigate the dynamic behaviors of the structure in which VRF Damper was installed. In addition, a hysteretic model for modeling the behaviors of

VRF Damper during earthquake was proposed and the results of experiment using the vibration table and the results of numerical analysis using the proposed hysteretic model were compared to evaluate its performance.

2. OVERVIEW OF THE VIBRATION EXPERIMENT FOR VARIABLE RESISTANCE FRICTION (VRF) DAMPER

2.1 Material Property of Test Specimen and Bolt Initial Tension

The material types and components used for Variable Resistance Friction (VRF) Damper experiment are: two T-shaped flanges (SS400) at the top and the bottom, two additional patches (SS400) and four M20 bolts (F10T). Between the T-shaped flanges and the patches, a high-strength aluminum plate (Al2017P), which was relatively less deformed by temperature-dependent friction, was used as aluminum abrasive. The material property of test specimen is shown in Table 1. Also, in order to limit the surface of friction to the space between the T-shaped flange and the aluminum abrasive, the path and the aluminum abrasive were shot-blasted to have the surface roughness of 50 μm or more, in order to ensure high friction. The aluminum abrasive was prepared to have upper part (t=5 mm: low-resistance part), lower part (t=2 mm: high-resistance part). As shown in Fig. 1, a slot with the width of 22 mm and the length of 62 mm was installed in the upper T-shape flange of VRF Damper and one with the width of 22 mm and the length of 92 mm was installed in the lower T-shape flange, to allow the maximum deformation of ±20 mm for the low-resistance part and ±35 mm for the high-resistance part. In order to create different slip resistances in the variable resistance friction damper, the bolt tension of 30 kN was introduced to each of two high-tension bolts in the low-resistance part, and 80 kN to each of two high-tension bolts in the high-resistance part. The bolts were tightened with a torque wrench at room temperature so that the same force could be applied to them.

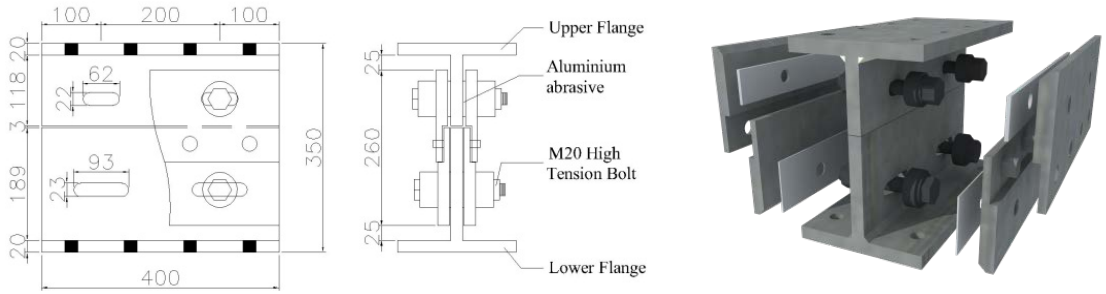

Figure 1. Variable resistance friction damper detail

Table 1. Material Property of the Specimen

Specimen	Material	Yield Strength (σ_y)	Tensile Strength (σ_u)	Elongation (ε_u)	Shear Yield Strength ($\sigma_y/\sqrt{3}$)
Aluminum Abrasive	A2017P	357.1	435.3	14.6	206.2
Body	SS400	397.6	589.0	45.6	244.7

2.2 Vibration Test using the Earthquake Simulation Device

In order to investigate the dynamic behaviors and performance of the proposed Variable Resistance Friction (VRF) Damper, two VRF Dampers were installed on the left and the right sides of a steel structure with SDOF and the vibration table test was carried out for the test setup. Detailed dimensions of the members of the test specimen are shown in Fig. 2 and, for all members, SS400 steel was used. The specimen columns were designed to be pin-ended so that they resisted against the vertical load only, and it was designed in a way that all horizontal loads were held by VRF Damper. Total weight used for the test was 176.4 kN made up of sixty 2.94 kN weights. As shown in Fig. 3, two accelerometer sensors were installed on the base beam to obtain test data, and two accelerometer

sensors and a displacement meter on the upper parts of front and rear frames. In addition, in order to measure the displacement of the entire VRF Damper and that of low-resistance and high-resistance parts, displacement meters were installed respectively.

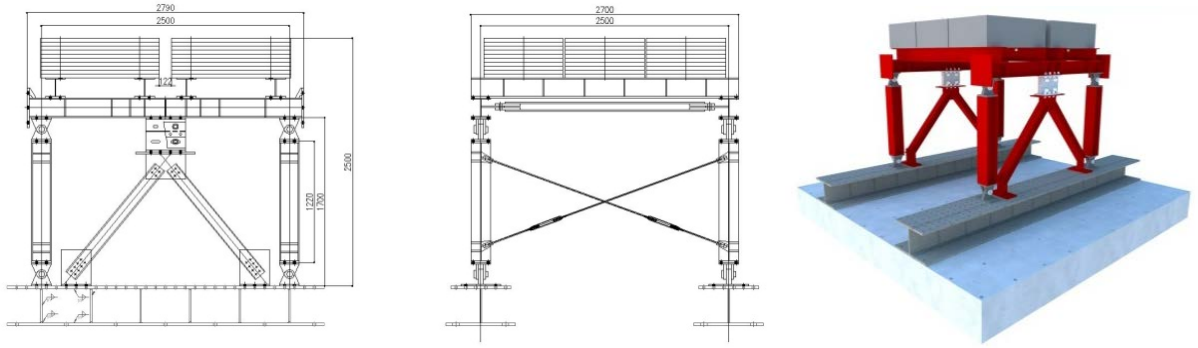

Figure 2. Test set-up

Photo 1. VRF Damper

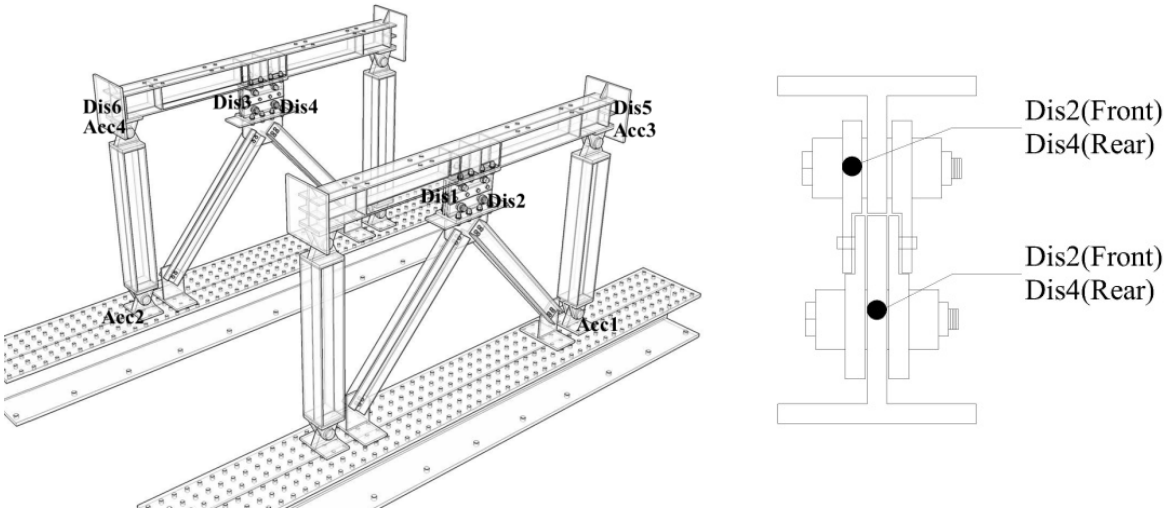

Figure 3. Detail of measurement position

Table 2. Details of Member

Member	Material	Size
Column	SS400	H200 x 200 x 8 x 12
Beam		H200 x 200 x 8 x 12
Brace		2-⊏125 x 65 x 6 x 8

2.3 Characteristics of Input Earthquake Waves

In order to evaluate the structural behavior and performance of VRF Damper, the vibration test was carried out on the vibration table using El Centro NS (1984), JMA Kobe NS earthquake waveform. Especially, in order to examine the performance of VRF Damper particularly by which only the low-resistance part reacts at a small-scale earthquake and both the low-resistance and the high-resistance parts react simultaneously at a large-scale earthquake, the earthquake scale was adjusted at the vibration table. The input values for earthquake waves used for the test and the elastic response spectra of the measured earthquake waves are shown in Fig. 4. Table 3 shows the scales of earthquake waves used for the test.

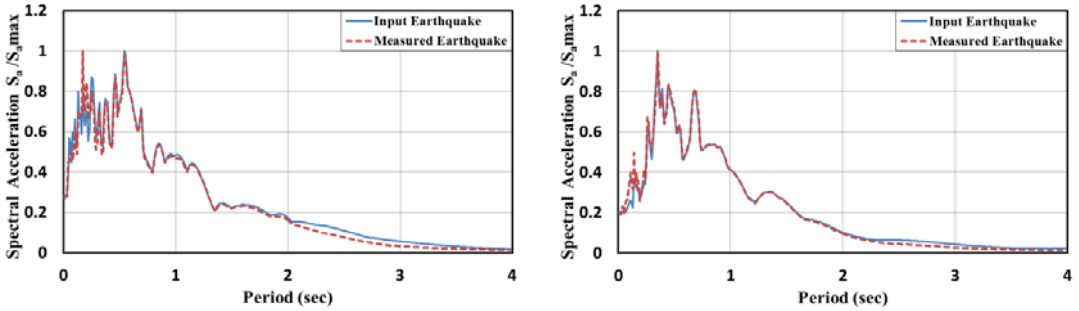

(a) El Centro Earthquake NS (b) Kobe Earthquake NS

Figure 4. Comparison of linear elastic response spectra of input and measured earthquake

Table 3. Overview of Test Specimen

Test Names	E.Q. Wave	Scale (%)	PGA (g)	Remarks
El-60	El Centro NS	60	0.15	Installation of Initial Tension
El-100		100	0.25	Reinstallation of Tension
El-180		180	0.45	Reinstallation of Tension
El-300		300	0.75	Reinstallation of Tension
Ko-60	JMA Kobe NS	60	0.48	Replacement of Aluminum Abrasive
Ko-100		100	0.801	Reinstallation of Tension

3. TEST RESULTS

3.1 Acceleration Response of the Structure

The acceleration response of each test specimen of the structures on which VRF Damper was installed was filtered through Low Pass Filter (cutting off 10 Hz or more), of which result is shown in Fig. 5.

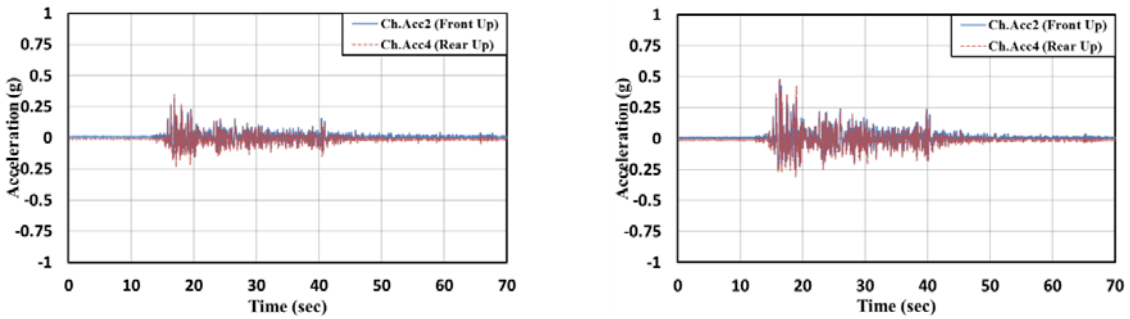

(a) El-60 (b) El-100

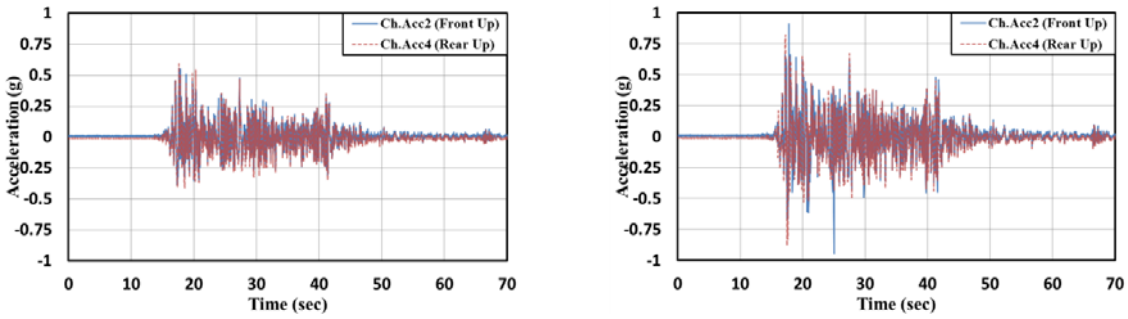

(c) El-180 (d) El-300

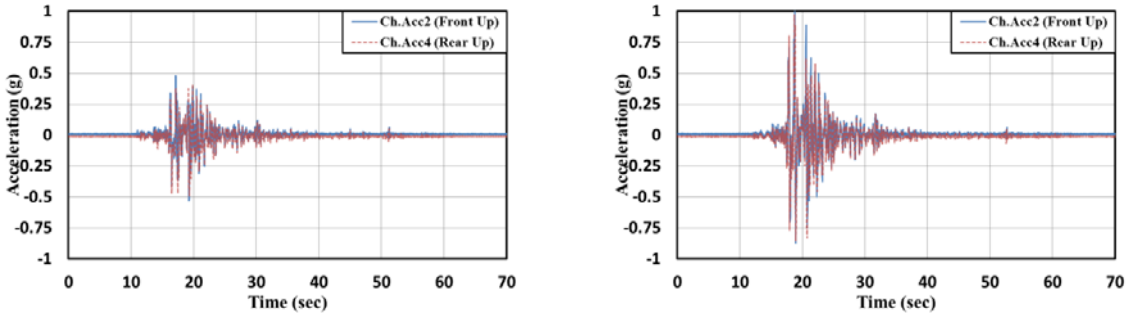

(e) Ko-60 (f) Ko-100

Figure 5. Roof response acceleration for each test type

3.2 Slip Load-Displacement Hysteretic Curve for Variable Resistance Friction Damper

As the columns of the test specimen for this study were pin-ended, the resistance to horizontal load was all held by the variable resistance friction damper. In this test, the mean value of accelerations measured at the upper part of each steel structure described in Section 3.1 was calculated and then multiplied by the upper part weight of 176.4 kN, to calculate the slip resistance of the damper. The overall displacement of the damper was obtained using the average value of the displacement response measured at the upper structure. Fig. 6 shows the slip resistance-displacement relationship for each test specimen. The initial stiffness measured at the initial tension of 30 kN at the low-resistance part bolt of El-60 and E1-100 test specimens was 280 kN/mm. For El-60, El-100, El-180 and Ko-60 test specimens, the behavior of the low-resistance part of the damper was obtained (about 60 kN) and for El-300 and Ko-100 test specimens, the behaviors of the low-resistance part and the high-resistance part (about 160 kN) were obtained. The relationship between the slip friction resistance F of the friction damper and the initial tension N of the bolt can be expressed as Equation (1).

$$F = m \cdot \mu \cdot N \tag{1}$$

where, F is the slip resistance; m the number of friction surfaces (2-surface friction); μ friction coefficient (=0.25); and N the sum of initial tensions of the bolts.

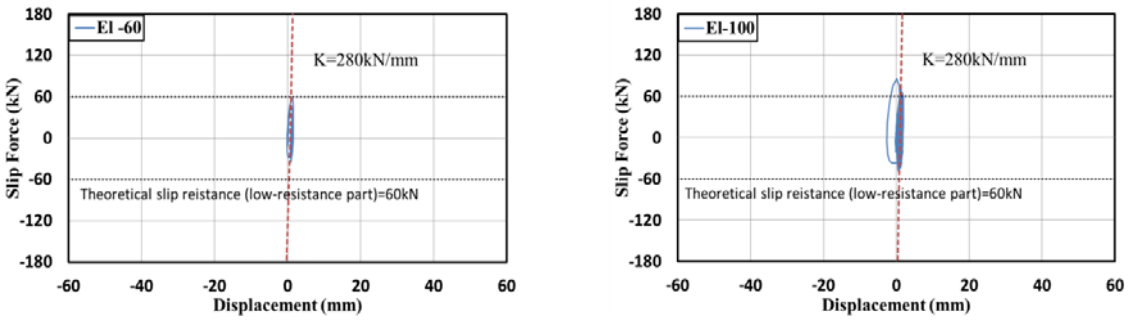

(a) El-60

(b) El-100

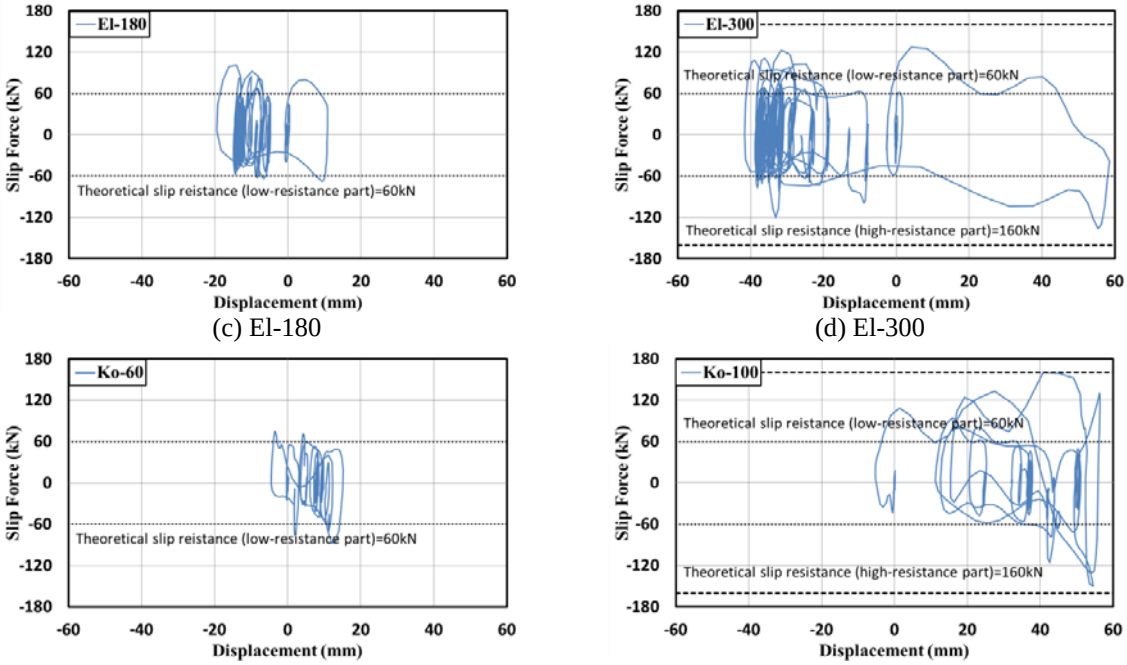

(c) El-180 (d) El-300

(e) Ko-60 (f) Ko-100

Figure 6. Slip force-displacement relationship for each test specimen

4. ANALYSIS OF SEISMIC RESPONSE OF SDOF STRUCTURE WITH VARIABLE RESISTANCE FRICTION DAMPER

4.1 Proposal of Hysteretic Behavior Model for VRF Damper

In order to verify the restoration characteristics of VRF Damper obtained through the test a proper restoration analysis model shown in Fig. 7 was proposed. According to this restoration characteristics model, the hysteretic behavior proceeds at the initial stiffness of K_1 until the primary yield and then proceeds at a constant resistance value (low-resistance part) once the primary yield is reached. Afterwards when Δ value is reached, it proceeds with deformation at the value of the secondary stiffness K_2 and when the secondary yield is reached, deformation continues with forming high-resistance part. When the load is reduced (speed is reversed), the primary stiffness is restored and when the reverse primary yield is reached, only deformation proceeds. When the displacement becomes 2Δ or bigger, the hysteretic behavior proceeds at the secondary initial stiffness K_2 and when the secondary yield is reached, only deformation proceeds. In order to examine the compatibility between the results of the vibration table test and the proposed hysteretic behavior model, a nonlinear-time history analysis was carried out for test specimens modeled into SDOF structures. For the hysteretic behavior characteristics of SDOF model, the initial tension of low-resistance part was estimated as 60 kN, that of high-resistance part as 160 kN, and the initial stiffness as 280 kN/mm; and the same conditions as those for the vibration table test were set. In addition, the damping coefficient for the entire structures was set as C=0.003. Especially, as for the characteristics of the input earthquake wave, the acceleration measured for each test specimen at the base beam of the vibration mentioned in table 3 above was used as the input earthquake wave. As for the numerical integration to solve the equation of motion, the central difference method was used.

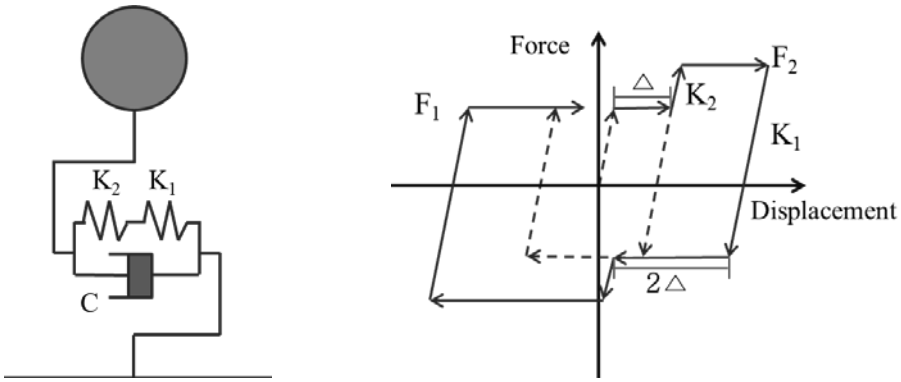

(a) SDOF Model (b) Damper Hysteresis Model

Figure 7. Proposed hysteretic behavior model for variable resistance friction damper

4.2 Comparison of the Analysis Results

Fig. 8 shows the comparison between the result of the vibration table test and that of the nonlinear time hysteretic analysis for the variable resistance friction damper.

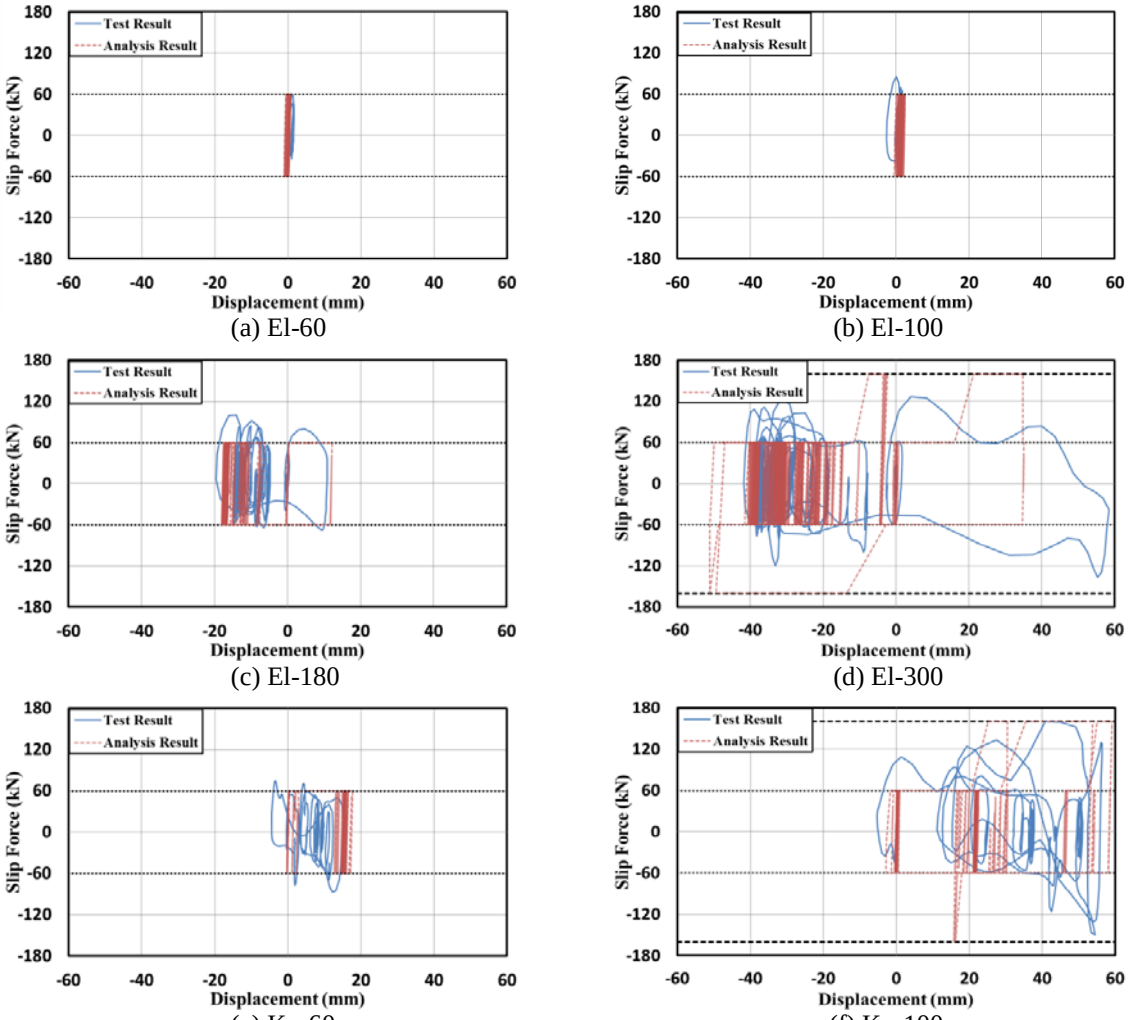

(a) El-60 (b) El-100

(c) El-180 (d) El-300

(e) Ko-60 (f) Ko-100

Figure 8. Hysteresis loop for analysis model

It is shown that the proposed restoration characteristics model can reproduce El-centro NS and JMA Kobe NS earthquake waves well. As shown in Fig. 8 (a), (b) and (e), the slip resistance and the displacement response of the low-resistance part are reproduced with a considerably high precision. Though there is a slight difference in the high-resistance part behavior section following the low-resistance part behavior section (displacement amplitude: -20 mm ~ +20 mm), it is clear that general response behavior for earthquakes is significantly reproduced. (Figure 10 (c), (d) and (f))

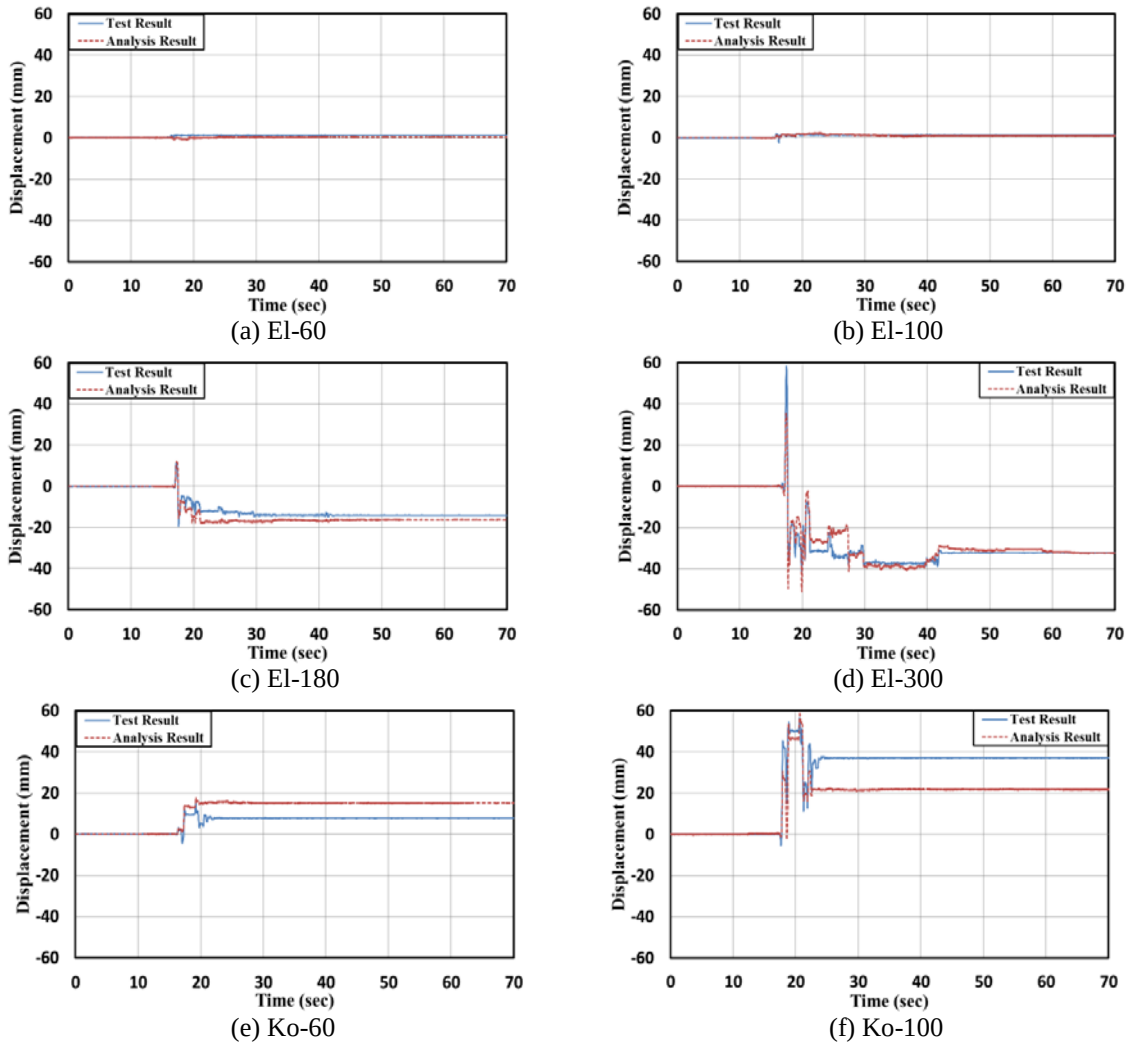

Figure 9. Roof displacement for analysis model

Fig. 9 shows the displacement-time hysteresis curves for the result of vibration table test and that of nonlinear-time hysteretic analysis. Through comparison of the results, it was confirmed that, despite slight difference in the displacement response at the time of high-resistance part behavior, the proposed hysteretic behavior model can reproduce general behaviors of the structure equipped with the variable resistance friction damper at the time of earthquake.

5. CONCLUSION

In order to understand dynamic behaviors of the variable resistance friction damper that can respond to the earthquake scale, the vibration test using the earthquake simulation device was carried out and the following conclusion was obtained:

1. The results of the vibration table test for the SDOF steel structure equipped with the damper confirmed that the low-resistance part and the high-resistance part of the damper reacted successively in response to the earthquake scale, and therefore it is possible to use the damper as an energy absorber at the time of earthquake.

2. A variable resistance hysteretic behavior model was proposed based on the result of the vibration table test, which could reproduce the low-resistance part and the high-resistance part of the variable resistance friction damper.

3. The result of the nonlinear-time history analysis for the SDOF steel structure based on the proposed hysteretic behavior model showed that the model could reproduce well the response characteristics of earthquakes.

ACKNOWLEDGEMENT

This research was by Basic Science Research Program through the National Research Foundation of Korea(NRF) funded by the Ministry of Education. Science and Technology(No. 2011-0020027) and (No.2011-0005818)

REFERENCES

Pall A S and Marsh C. (1982). Seismic Response of Friction Damped Braced Frames. *Journal of Structural Division*, ASCE. **108:ST6**, 1313-1323.

KOBORI Tohru. (1987). Application of friction damper to highrise steel Building(part1~5). *Summaries of technical papers of Annual Meeting Architectural Institute of Japan. B*. **Structures I.**

Gregorian, C.E. et al. (1993). Slotted Bolted Connection Energy Dissipaters. *Earthquake Spectra*. **9:FD1-3**, 491-504.

Yu Kikuchi, Mitsuru Sano, Takashi Kageyama, Suzui Yasumasa and Shirai Kazutaka. (2012). Development of Friction Damper with Displacement Dependent Variable Damping Force Characteristics, *Journal of structural and building science*, **18:38**, 85-90.

Soon T T and Spencer Jr B F. (2002). Supplemental Energy Dissipation: State-of-the-Art and State-of-the-Practice. *Engineering Structure*. **24:FD1-3**. 243-259.

WU Bin, ZHANG Ji-gang and OU Jin-ping. (2004). The Analysis and Comparison of Seismic Performance of Structures with Three Types of Dampers. *World Earthquake Engineering*. **20:FD1-1**. 21-26.

FUKAZAWA Kyozo , HASEGAWA Yutaka , TANAHASHI Yoshiyuki and MIYOSHI Masakazu. (2007). Development of Detached House Damping using CFD friction damper, *Journal of structural and construction engineering. Transactions of AIJ*. **13:26**, 551-556.

KASAI Kazuhiko , WADA Akira , SAKATA Hiroyasu , MIDORIKAWA Mitsumasa , OOKI Yoji and NAKAGAWA Toru. (2005). Shaking Table Tests of Wood Frames with Deformation Dependent Dampers, *Journal of structural and construction engineering. Transactions of AIJ*. **594**. 101-110.

YOKOUCHI Hajime , KITAJIMA Keiji , NAKANISHI Mitsukazu , ADACHI Hiromi and AOYAMA Hiroyuki. (2008). Earthquake Response Characteristics of an Existing R/C Building Retrofitted with Friction Dampers, *Journal of structural and construction engineering. Transactions of AIJ*. **73:628.** 947-955.